Distribution and inventory of anthropogenic CO2 in the Southern Ocean: Comparison of three data-based methods

Claire Lo Monaco, Catherine Goyet, Nicolas Metzl, Alain Poisson, Franck Touratier

Distribution and inventory of anthropogenic CO_2 in the Southern Ocean: Comparison of three data-based methods

C. Lo Monaco,[1] C. Goyet,[2] N. Metzl,[1] A. Poisson,[1] and F. Touratier[2]

[1] The Southern Ocean is thought to play an important role in the context of global warming and anthropogenic emissions of CO_2 due to its high sensitivity to both climate change and changes in the carbon cycle. Assessing the penetration of anthropogenic CO_2 (C^{ant}) into the Southern Ocean is therefore highly relevant to reduce the uncertainties attached to both the present knowledge of anthropogenic carbon inventories and predictions made by current ocean carbon models. This study compares different data-based approaches for estimating the distribution of C^{ant} in the ocean: a recently developed method based on the composite Tracer Combining Oxygen, Inorganic Carbon, and Total Alkalinity (TrOCA) and the "historical" back-calculation methods (the so-called ΔC^* and preformed dissolved inorganic carbon methods). Note that the back-calculation technique requires special care when used in the Southern Ocean, where surface oxygen can significantly deviate from equilibrium with the atmosphere. All three methods were applied to data collected at the Indian-Atlantic boundary (WOCE line I6), where significant transient tracer concentrations were observed in deep and bottom waters. North of 50°S, distribution and inventories of C^{ant} are coherent with previous data-based and model estimates, but we found larger storage of C^{ant} south of 50°S as compared to the midlatitude region. In that, our results disagree with most previous estimates and suggest that the global inventory of anthropogenic CO_2 in the Southern Ocean could be much larger than what is currently believed.

1. Introduction

[2] The carbon cycle is closely link to climate: on the one hand, the uptake of CO_2 by the ocean regulates the accumulation of this greenhouse gas in the atmosphere thus controlling global warming but, on the other hand, the rate of CO_2 uptake by the ocean is in turn affected by climate change (through changes in biogeochemical and physical ocean processes). In the context of future climate change, studies of the carbon cycle in the ocean are needed in order to assess its present state and predict how it will evolve in the future in relation to climate. The Southern Ocean, in particular, was found to be very sensitive to past naturally occurring climate changes [e.g., *Watson et al.*, 2000] and it is expected to be also very sensitive in the future [e.g., *Bopp et al.*, 2001].

[3] Ocean general circulation models (GCMs) are currently used together with ocean carbon models in order to predict the evolution of the carbon cycle in the ocean, to quantify the impact of high CO_2 on ocean chemistry and marine biology and to determine the consequences for our future climate. Ocean models are also used to test the effectiveness of different carbon management strategies aiming to regulate the amount of CO_2 in the atmosphere, such as the Intergovernmental Panel on Climate Change (IPCC) scenario (reduction of anthropogenic CO_2 emissions), or purposeful ocean carbon sequestration experiments proposed to accelerate the uptake of CO_2 by the ocean (e.g., direct injection of CO_2 or iron fertilization). It then appears that ocean GCMs are very useful tools to study issues relevant to the carbon-climate system. However, although current ocean models generally agree on the total amount of anthropogenic CO_2 (C^{ant}) taken up by the ocean, different models present dramatic differences in regional predictions. In the framework of Ocean Carbon Model Intercomparison Project (OCMIP1 [*Orr et al.*, 2001]), for example, four different ocean carbon GCMs agree on a global ocean uptake of 1.85 ± 0.35 GtC/yr for the 1980s but different regional patterns were predicted for both the uptake and the storage of C^{ant}, with the largest disagreements found in the southern high latitudes. Disagreements in the penetration of C^{ant} into the deep Southern Ocean result in large uncertainties in the inventories of C^{ant} south of 50°S. In the South Atlantic, for example, the four OCMIP1 models predict C^{ant} inventories ranging between 10 and 50 mole of C/m^2 [*Orr et al.*, 2001]. Because the Southern Ocean is thought to be very sensitive to climate change, it is of primary importance to validate ocean models especially in

[1] Laboratoire d'Océanographie et du Climat: Expérimentations et Approches Numériques, Université Pierre et Marie Curie, Paris, France.
[2] Laboratoire de Biophysique et Dynamique des Systèmes Intégrés, Université de Perpignan, Perpignan, France.
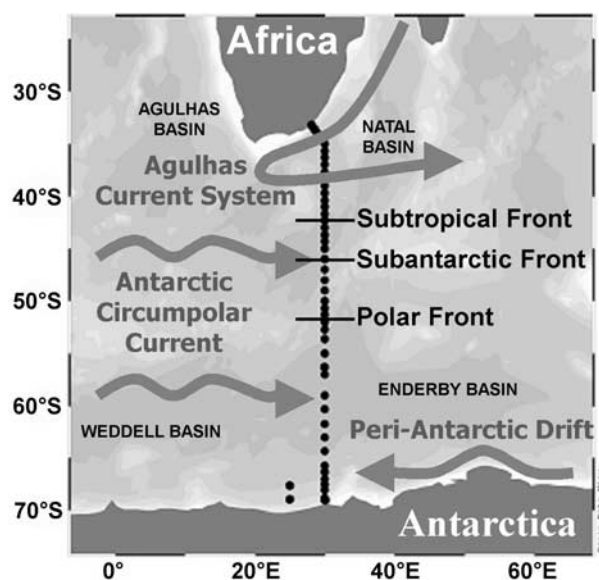
Figure 1. Map showing the location of stations visited in 1996 during CIVA-2 cruise (WOCE line I6). Only stations where dissolved inorganic carbon (DIC) and alkalinity data were collected are shown.

this region [*Friedlingstein et al.*, 2003]. However, uncertainties attached to global models are difficult to assess south of 50°S since estimates of C^{ant} using data-based methods also show large disagreements in this region [e.g., *Poisson and Chen*, 1987; *Gruber*, 1998; *Sabine and Feely*, 2001; *Sabine et al.*, 2002; *Lo Monaco et al.*, 2005].

[4] Different data-based methods exist to estimate the total amount of anthropogenic CO$_2$ (C^{ant}) accumulated in the ocean. The "historical" methods are based on the back-calculation technique which was proposed independently by *Brewer* [1978] and *Chen and Millero* [1979]. The initial method, hereafter referred to as the preformed dissolved inorganic carbon (DIC) (C^0) method, has been tested in various regions of the world ocean by A. Chen and coworkers [e.g., *Chen*, 1982; *Poisson and Chen*, 1987; *Chen*, 1993] and more recently in the North Atlantic Ocean by *Goyet et al.* [1998] and *Körtzinger et al.* [1998, 1999]. *Gruber et al.* [1996] developed the ΔC* method, a different back-calculation technique based on the use of transient tracers. The ΔC* method was first tested in the North Atlantic Ocean by *Gruber et al.* [1996] and later applied globally in the Atlantic [*Gruber*, 1998; *Lee et al.*, 2003], as well as in the Indian and Pacific Oceans [*Sabine et al.*, 1999, 2002]. The back-calculation technique is based on a number of assumptions and simplified biogeochemical concepts whose validity has been widely discussed in the past [e.g., *Shiller*, 1981, 1982]. The ΔC* method has been further improved by several authors in order to relax some of the assumptions [e.g., *Holfort et al.*, 1998; *Pérez et al.*, 2002], but other problems persist, such as the assumption of oxygen equilibrium in surface waters. In the Southern Ocean where ice coverage reduces the air-sea gas exchanges, the issue of oxygen equilibrium is of primary importance and should not be neglected [*Ito et al.*, 2004]. In a previous study, a regional C^{ant} calculation along WOCE

line I6 (30°E), it was found that when oxygen disequilibrium under the ice is taken into account in both the C^0 and ΔC* methods, the distribution of C^{ant} becomes much better correlated with chlorofluorocarbons (CFCs) and C^{ant} inventories become higher at high latitudes than at midlatitudes [*Lo Monaco et al.*, 2005]. This finding is opposed to what is usually obtained by ocean models and data-based studies [e.g., *Orr et al.*, 2001; *Sabine et al.*, 2004]. As a consequence, if the feature obtained along 30°E is representative of other areas in the Southern Ocean, the global ocean budget of anthropogenic carbon could be much larger than what is currently believed. The objective of the present study is to confirm these results using different data-based methods.

[5] Recently, three independent methods have been developed to determine C^{ant} in which no assumption is done about oxygen saturation in surface waters: the MIX method [*Goyet et al.*, 1999], a CFC-based method [*Hall et al.*, 2004], and the TrOCA method [*Touratier and Goyet*, 2004b]. These different approaches are an alternative to the "historical" back-calculation technique and may prove particularly useful in the Southern Ocean, but to date they have only been used north of 50°S in the Atlantic and Indian Oceans. In the present study we have chosen one of these approaches, the TrOCA method, to be tested for the first time in the southern high latitudes. Distribution and inventories of C^{ant} estimated in the Southern Ocean along WOCE line I6 using the TrOCA method are compared with C^{ant} estimates obtained along the same line using the "historical" C^0 and ΔC* methods.

2. Method

[6] Data used in this study were collected in the Southern Ocean during the French cruise CIVA-2 conducted in February–March 1996 (WOCE line I6 (Figure 1)). Information about sampling protocols and measurement techniques is given by *Lo Monaco et al.* [2005] with a description of the main hydrological features observed in this region. The ΔC*, C^0, and TrOCA methods have been described in detail by *Gruber et al.* [1996], *Lo Monaco et al.* [2005], and *Touratier and Goyet* [2004b], respectively. Here we briefly present the principle of each approach and indicate the parameterizations used in our study. Then, all three methods are put together in order to highlight similarities and differences that are discussed later.

2.1. Tracer Combining Oxygen, Inorganic Carbon, and Total Alkalinity (TrOCA) Method

[7] Very recently, *Touratier and Goyet* [2004b] proposed a new approach to estimate C^{ant} based on the quasi-conservative Tracer Combining Oxygen, Inorganic Carbon, and Total Alkalinity (TrOCA) [*Touratier and Goyet*, 2004a]). TrOCA is derived in the same manner as tracers NO or PO defined by *Broecker* [1974]. The Redfield ratios C/O$_2$ and N/O$_2$ are used so that any change in dissolved inorganic carbon (DIC) or total alkalinity (TA) induced by biological processes are balanced by change in oxygen (O$_2$), as follows:

$$\text{TrOCA} = \text{O}_2 + \frac{\text{DIC} - 0.5\text{TA}}{r_{\text{C/O}} + 0.5r_{\text{N/O}}}. \tag{1}$$
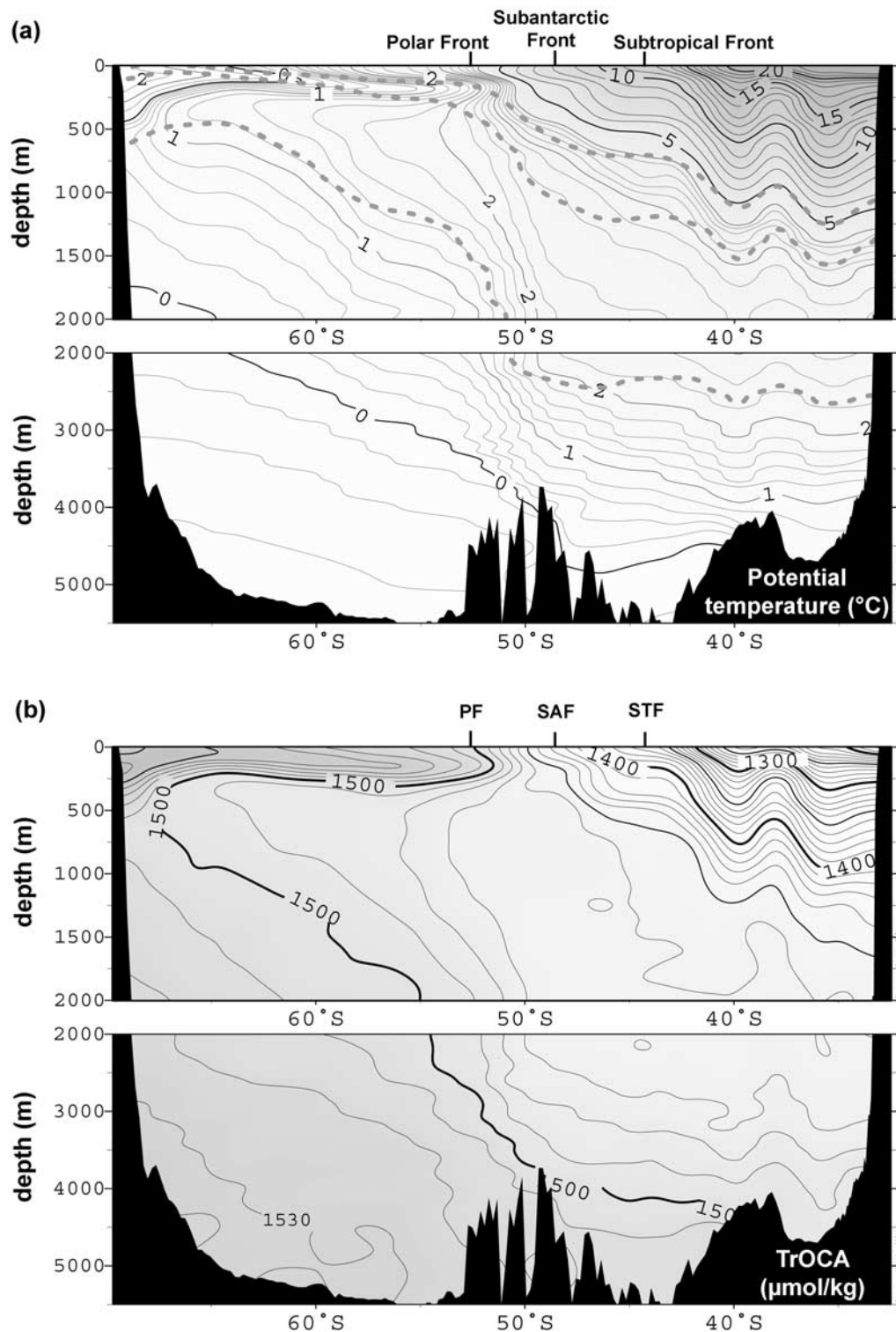
Figure 2. Distribution of potential temperature (θ) and Tracer Combining Oxygen, Inorganic Carbon, and Total Alkalinity (TrOCA) along 30°E in the Southern Ocean (WOCE line I6). Shaded dashed lines in Figure 2a indicate the 27.25, 27.5, and 27.8 potential density levels (σ_θ).

Touratier and Goyet [2004a] have demonstrated that TrOCA is conservative, except in the upper layer where air-sea gas exchange can occur, just like other tracers such as salinity, temperature, NO or PO. The tracer TrOCA also presents the advantage of being time-dependent (like

transient tracers) since TrOCA increases in response to the increase in anthropogenic CO_2 (C^{ant}). If we assume that O_2 and TA are not significantly affected by anthropogenic forcing and that the ocean operates at a steady state, the increase in TrOCA with time is directly related to the
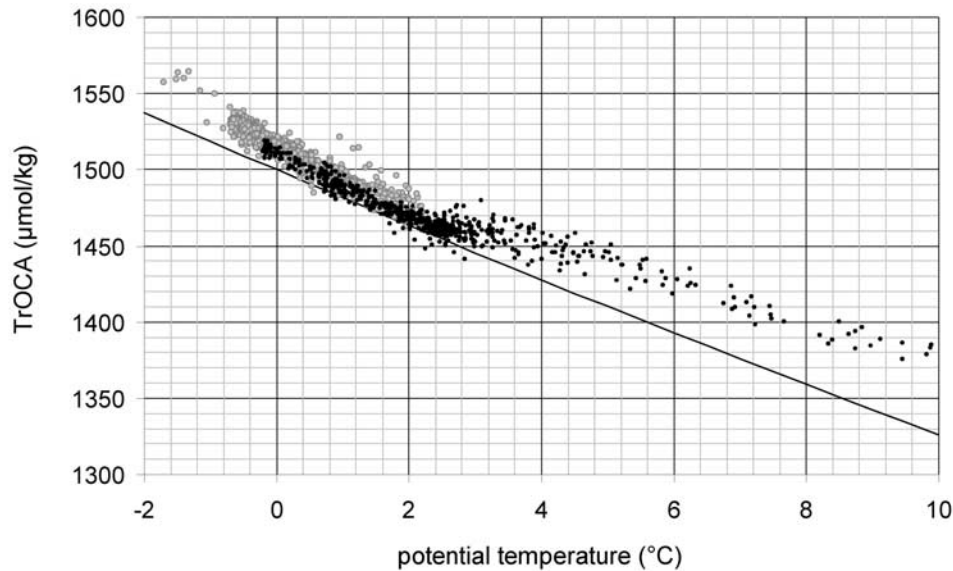
Figure 3. Relationship observed between potential temperature (θ) and the tracer TrOCA along 30°E in the Southern Ocean (WOCE line I6). Data presented in the plot are for waters below the maximum mixed layer depth: 500 m north of the subantarctic front (black dots) and 200 m in the south (shaded dots). The preindustrial TrOCA estimated with model terms $A = 1500$ and $B = 81.1$ is also shown (equation (4)) (black line).

accumulation of C^{ant} into the ocean. On the basis of this approach, the following formulation is used for C^{ant}:

$$C^{ant} = (r_{C/O} + 0.5r_{N/O})(TrOCA - TrOCA^0), \qquad (2)$$

where TrOCA^0 is the preindustrial TrOCA. *Touratier and Goyet* [2004a] showed that the distribution of TrOCA in the ocean is well correlated with the potential temperature and proposed to deduced TrOCA^0 from a single temperature relationship.

2.1.1. Distribution of TrOCA Along 30°E

[8] We calculated TrOCA in the Southern Ocean using CIVA-2 data collected along 30°E (WOCE line I6) and the same Redfield ratios as by *Touratier and Goyet* [2004a, 2004b], i.e., C/O$_2$ = 123/165 and N/O$_2$ = 17/123 [*Körtzinger*, 2001]. The following formulation was used for TrOCA:

$$TrOCA = O_2 + 1.2DIC - 0.6TA. \qquad (3)$$

The distribution of TrOCA along WOCE line I6 is presented conjointly with potential temperature (θ) in Figure 2. As a general rule, TrOCA increases with decreasing temperature: TrOCA is low in warm surface waters and increases toward the south and with depth. North of 50°S, TrOCA ranges between 1250 and 1520 μmol/kg and is associated with a large range in temperature (−0.2°–23°C). High vertical gradients of TrOCA and potential temperature are observed down to 1500 m. Below the thermocline (θ < 4°C), TrOCA is rather homogeneous with values between 1450 and 1460 μmol/kg for potential temperatures ranging from 2.5°C to 4°C. Deeper in the water column, TrOCA increases slightly up to 1470 μmol/kg in North Atlantic Deep Water (NADW) centered around 3000 m in the Agulhas-Natal

basin. The highest TrOCA values (>1500 μmol/kg) are found in Antarctic Bottom Water (AABW) flowing north of the Indian-Atlantic ridge. South of 50°S, the reduced range in temperature (−2°–2°C) is correlated with a reduced range in TrOCA (1480–1570 μmol/kg). TrOCA reaches its maximum values in the coldest waters: the Winter Water centered around 200 m (>1550 μmol/kg) and AABW flowing along the Antarctic slope and in the Weddell-Enderby basin (>1530 μmol/kg). Lower TrOCA values (1480–1500 μmol/kg) are found in the maximum temperature layer which characterizes the upper Circumpolar Deep Water (upper CDW), a mixture of deep waters flowing out of the Atlantic, Indian and Pacific basins [*Rintoul et al.*, 2001]. These deep outflow waters, the oldest waters found south of 50°S, should contain few anthropogenic CO$_2$. When approaching the Antarctic continent, deep waters mix with younger waters of southern origin to form either the Modified CDW (M-CDW) or Antarctic Bottom Water (AABW). The spreading of both M-CDW and AABW contributes to the ventilation of the deep Southern Ocean [*Orsi et al.*, 2002]. Interestingly, TrOCA increases southward due to the influence of the cold southern waters with higher TrOCA and probably higher concentrations of C^{ant} (WW and AABW). The tracer TrOCA therefore provides useful information to discriminate between the recently ventilated CDW and the old upper CDW. In that, TrOCA is complementary to other tracers such as NO or PO which only provide information on the origin of water masses.

[9] The increase of TrOCA with decreasing temperature is illustrated in Figure 3. *Touratier and Goyet* [2004a] found that for latitudes ranging between 50°N and 50°S, a linear or sigmoid relationship could be used to correlate TrOCA with temperature. They did not discuss this relationship for the southern high latitudes because they have used a data set

which provides few observations south of 50°S (CARINA database). Using WOCE data collected in the South Atlantic (including CIVA-2 cruise), we find a good relationship between potential temperature and TrOCA for both the water masses north and south of the polar front.

2.1.2. Estimation of the Preindustrial TrOCA (TrOCA^0)

[10] If we assume that the relationship observed between TrOCA and temperature had remained constant during the preindustrial era, waters formed more than 200 years ago can be used as a reference to deduce the preindustrial TrOCA (TrOCA^0). *Touratier and Goyet* [2004b] showed that for potential temperature (θ) ranging between -2°C and 30°C, a theoretical relationship, an exponential function of the form $A \exp(-\theta/B)$, can be used to express TrOCA^0. In *Touratier and Goyet* [2004b], the model terms $A = 1505.04$ (± 0.46) and $B = 89.04$ (± 1.50) were determined from data collected in deep and bottom waters ($\theta < 2.5$°C) in the South Atlantic Ocean (20°−40°S). Model terms A and B have been reevaluated in the North Indian deep and bottom waters ($\theta < 7$°C) using WOCE data collected along line I1. The new values obtained for A and B are rather close to the early prediction, but a much better precision is achieved: $A = 1500$ (± 0.28) and $B = 81.1$ (± 0.34). This new parameterization leads to similar TrOCA^0 values in the coldest waters but slightly lower values in warmer waters (<10 µmol/kg lower for $\theta < 3$°C). As this parameterization also leads to a worldwide coherence, checked using a world data set (Glodap, http://cdiac. ornl.gov/oceans/glodap), the following equation was used to calculate TrOCA^0 in our study:

$$TrOCA^0 = 1500 \exp(-\theta/81.1). \qquad (4)$$

Although the empirical terms A and B were obtained within a reduced range of temperature, the use of a theoretical function of the form $A \exp(-\theta/B)$ ensures the validity of equation (4) for temperatures up to 30°C. We used the standard deviations of A (± 0.28) and B (± 0.34) to evaluate the statistical error associated with the calculation of TrOCA^0 within the range -2°C to 30°C [see *Touratier and Goyet*, 2004b, equation (6)]. The error in TrOCA^0 is very small in cold waters (<0.6 µmol/kg for $\theta < 7$°C) and increases slightly in warmer waters (up to 1.6 µmol/kg at 30°C).

[11] Figure 3 compares TrOCA and TrOCA^0 calculated along 30°E in the Southern Ocean (CIVA-2 data). For a given temperature, the difference observed between TrOCA and TrOCA^0 is proportional to the amount of C^{ant} accumulated in the water mass (equation (2)). For example, one would expect a significant storage of C^{ant} in the cold waters of the Southern Ocean ($\theta < 0$°C) where CFC concentrations are high [*Lo Monaco et al.*, 2005] and where TrOCA increased by 10−30 µmol/kg since the preindustrial era (Figure 3).

2.2. Back-Calculation Methods

[12] The back-calculation technique was first proposed independently by *Brewer* [1978] and *Chen and Millero* [1979]. It is based on the idea that the CO$_2$ in "excess," or anthropogenic CO$_2$ imprinted within a water mass when it was formed, can be deduced from DIC measurements by going back into the water mass history. When a water mass

is formed, it loses contact with the atmosphere with an initial or preformed DIC concentration (C^{0,form}). Along the way to the ocean interior, water masses are further supplied with DIC through biological activity. C^{0,form} can be estimated by retrieving the biological contribution (C^{bio}) from DIC measurements (C^{0,form} = DIC − C^{bio}). For water masses formed during the industrial era, C^{0,form} can be decomposed into a "natural," or preindustrial, component (C^{0,PI}) and the anthropogenic CO$_2$ (C^{ant}). It then appears that C^{ant} can be deduced from DIC measurements if we can accurately estimate C^{bio} and C^{0,PI}, as follows:

$$C^{ant} = DIC - C^{bio} - C^{0,PI}. \qquad (5)$$

2.2.1. Formulation of the Biological Contribution (C^{bio})

[13] When a water parcel leaves the surface, its initial DIC content increases through organic matter remineralization and carbonate dissolution. According to *Brewer* [1978] and *Chen and Millero* [1979], this biogenic DIC can be estimated from changes in alkalinity (ΔTA) and oxygen (ΔO$_2$) with the use of the Redfield ratios ($r_{C/O}$ and $r_{N/O}$):

$$C^{bio} = 0.5\Delta TA + (r_{C/O} + 0.5 r_{N/O})\Delta O_2. \qquad (6)$$

[14] ΔTA is the difference between measured alkalinity (TA) and preformed alkalinity (TA^0). If we assume that ocean physics operate in a steady state and that alkalinity is not affected by the input of anthropogenic CO$_2$, ΔTA is the increase in alkalinity resulting from biological processes only and TA^0 remains constant with time. TA^0 is predicted from an empirical relationship linking surface alkalinity with temperature, salinity and the conservative tracer PO (PO = O$_2$ + 170PO$_4$ [*Broecker*, 1974]). Note that two relationships are required in our study because water masses observed along 30°E have two different origins (Southern Ocean or North Atlantic). Relationships used in this study are those estimated by *Lo Monaco et al.* [2005].

[15] Apparent oxygen utilization (AOU) can be used for ΔO$_2$ in regions where surface oxygen is close to equilibrium with the atmosphere. AOU is the difference between oxygen saturation (calculated after *Benson and Krause* [1980]) and measured oxygen (AOU = O$_2^{sat}$ − O$_2$). When using the concept of AOU it is assumed that surface oxygen is close to equilibrium, which is true in most of the world ocean during winter because oxygen exchange at the air-sea interface are very fast. In ice covered regions, however, air-sea fluxes are considerably reduced and oxygen concentration under the ice can significantly deviate from saturation. In the Southern Ocean the upwelling of old deep waters with low oxygen content results in a systematic oxygen depletion in surface waters covered with ice [*Ito et al.*, 2004]. *Anderson et al.* [1991] calculated that Ice Shelf Water (ISW) involved in the formation of Antarctic deep and bottom waters left the surface of the Weddell Sea with a mean oxygen depletion of 12%. This number is in agreement with measurements in the Winter Water (WW) of the Weddell Sea [*Weiss et al.*, 1979; *Poisson and Chen*, 1987] and under the ice in Prydz Bay [*Gibson and Trull*, 1999], another probable site for dense water formation [e.g., *Mantisi et al.*, 1991; *Wong et al.*, 1998]. In a previous study, we showed that oxygen saturation is an important

issue in the Southern Ocean [*Lo Monaco et al.*, 2005] and proposed to correct the oxygen saturation value calculated in ISW and WW for a mean undersaturation $\alpha = 12\%$. The oxygen saturation correction is propagated into the deep ocean using the mixing ratio of ISW and WW (k). The following formulation is used for oxygen utilization:

$$\Delta O_2 = (1 - \alpha k)O_2^{sat} - O_2^m. \qquad (7)$$

Ratio k is determined using a mixing model described by *Lo Monaco et al.* [2005] based on the optimum multiparametric (OMP) analysis first proposed by *Tomczak* [1981] and further developed in many studies [e.g., *Coatanoan et al.*, 1999].

2.2.2. Estimation of the Preindustrial Preformed DIC ($C^{0,PI}$)

[16] Various techniques have been proposed to estimate the preindustrial preformed DIC ($C^{0,PI}$). It is not clear from the literature whether one of these techniques is more reliable than the other, each one having its own caveats in different regions of the world ocean [e.g., *Wanninkhof et al.*, 1999; *Sabine and Feely*, 2001; *Wallace*, 2001a, 2001b]. In *Lo Monaco et al.* [2005], however, we argued that for the high-latitude regions where dense water mass formation occurs the C^0 method has proved to give better results than the ΔC^* method in reproducing the deep penetration observed with other transient tracers such as CFCs.

[17] In the initial method, the C^0 method, $C^{0,PI}$ is estimated by using an old water as a reference, i.e., a water mass that last lost contact with the atmosphere during the preindustrial era and therefore contains a priori no anthropogenic CO_2. The preformed DIC calculated within this particular water mass ($[C^{0,form}]_{REF} = [DIC - C^{bio}]_{REF}$) is an estimation of the preindustrial preformed DIC in the formation region of the reference water ($[C^{0,PI}]_{REF}$). In order to estimate $C^{0,PI}$ in any region we must include a term accounting for regional differences (ΔC^0):

$$C^{0,PI} = [C^{0,PI}]_{REF} + \Delta C^0 = [DIC - C^{bio}]_{REF} + \Delta C^0. \qquad (8)$$

ΔC^0 is the difference between C^0 in any region and C^0 in the formation region of the reference water. We assume that this difference has remained constant since the preindustrial era and determine ΔC^0 using preformed DIC concentrations currently observed in the respective regions ($\Delta C^0 = C^{0,obs} - [C^{0,obs}]_{REF}$). The following formulation is used to estimate $C^{0,PI}$ in equation (5):

$$C^{0,PI} = C^{0,obs} + [DIC - C^{bio} - C^{0,obs}]_{REF}. \qquad (9)$$

$C^{0,obs}$ is the contemporary preformed DIC deduced from temperature, salinity and PO. As for alkalinity, two relationships are required to predict preformed concentrations in water masses originating from either the Southern Ocean or the North Atlantic. Relationships used in this study are those estimated by *Lo Monaco et al.* [2005]. The other three terms constitute the reference ($\Delta C^{0,REF}$). Calculation of the reference is detailed in section 2.2.3.

[18] The ΔC^* method is also based on equation (5) and the biological contribution (C^{bio}) is estimated in the same manner as in the C^0 method using equation (6). The only

difference with the initial C^0 method is the way $C^{0,PI}$ is estimated. *Gruber et al.* [1996] proposed to use the following expression for C^{ant}:

$$C^{ant} = DIC - C^{bio} - (C^{eq,280} + \Delta C^{dis}), \qquad (10)$$

where $C^{eq,280}$ is the DIC in equilibrium with the preindustrial atmosphere estimated as a function of salinity, temperature, alkalinity and atmospheric CO_2 (280 ppm). The first three terms on the right-hand side in equation (10) make up the quasi-conservative tracer ΔC^* [*Gruber et al.*, 1996]. The last term, ΔC^{dis} is the air-sea disequilibrium of CO_2. The assumption is made that ΔC^{dis} has remained more or less constant within the formation region of a particular water mass and that water masses are predominantly transported along isopycnal surfaces in a steady state ocean (i.e., ΔC^{dis} is constant along isopycnal surfaces). ΔC^{dis} is determined as a function of potential density (σ_θ) in two different manners. For old deep waters ΔC^{dis} can be deduced from the mean ΔC^* value calculated along isopycnal surfaces in the region a priori free of anthropogenic CO_2 ($C^{ant} = 0$ in equation (10)):

$$\Delta C^{dis} = \Delta C^{*,REF} = [DIC - C^{bio} - C^{eq(280)}]_{REF}. \qquad (11)$$

For shallower waters, no portion of the isopycnal surface can be assumed to be free of anthropogenic CO_2 (e.g., Antarctic Intermediate Water). In that case the air-sea disequilibrium of CO_2 (ΔC^{dis}) in the formation region is the difference between the calculated preformed DIC ($DIC - C^{bio}$) and DIC in equilibrium with the atmospheric CO_2 at the time of water mass formation ($C^{eq(t)}$). ΔC^{dis} is then deduced from the mean $\Delta C^{*(t)}$ defined along isopycnal surfaces as follows:

$$\Delta C^{dis} = \Delta C^{*(t)} = DIC - C^{bio} - C^{eq(t)}. \qquad (12)$$

$C^{eq(t)}$ can be calculated in the same manner as $C^{eq(280)}$ if the atmospheric CO_2 concentration at the time of water mass formation is known. *Gruber et al.* [1996] proposed to use transient tracers to determine the time of water mass formation (CFC-based age method for example) and the associated level of atmospheric CO_2.

[19] In this study we used the air-sea CO_2 disequilibrium values published by *Sabine et al.* [1999, Tables 2 and 3]. These numbers are adequate for our study since they were calculated from WOCE data collected in the Indian Ocean. The CO_2 disequilibrium calculated by *Sabine et al.* [1999] along shallow isopycnal surfaces ($\sigma_\theta < 27.25$) range from -1.3 μmol/kg at the surface down to -19.5 μmol/kg at the base of the thermocline (mean $\Delta C^{*(t)}$). Between the isopycnal 27.25 and 27.5, *Sabine et al.* [1999] used a combination of the mean $\Delta C^{*(t)}$ and ΔC^* to estimate the disequilibrium ($\Delta C^{dis} = -6.3$ to -9.1 μmol/kg). In deeper waters, below the 27.5 isopycnal and where CFCs are below a reasonable blank (CFC-12 < 0.005 pmol/kg), *Sabine et al.* [1999] used the mean ΔC^* value calculated in this region ($\Delta C^{*,REF}$) to estimate ΔC^{dis} and obtained values ranging from -9.3 to -18.6 μmol/kg. Note that in the deepest waters ($\sigma_\theta > 27.8$) ΔC^{dis} is set to the constant value of

Table 1. Random Errors Estimated for Parameters Used in the Calculation of C^{ant} [a]

Parameters	Measurements			Predictions					
	O$_2$	TA	DIC	O$_2^{sat}$	TA^0	C^{0,obs}	ΔC^{0,REF}	ΔC^{dis}	TrOCA^0
Random errors, μmol/kg	0.3	1.9	1.9	4.6	5.5	6.3	3.0	0.5	1.6

[a]Error estimates are from *Lo Monaco et al.* [2005], except for ΔC^{dis} [*Sabine et al.*, 1999] and TrOCA^0 (this study).

−18.6 μmol/kg because the mean ΔC* remains relatively constant in deep and bottom waters.

2.2.3. Reference Water

[20] As for the TrOCA approach, a preindustrial reference is required in order to estimate C^{0,PI} in the back-calculation methods. For the ΔC* method, the reference term ΔC*^{,REF} is calculated in deep and bottom waters of the Indian Ocean where CFCs are below the detection limit. For the C^0 method, we choose to calculate the reference term ΔC^{0,REF} in North Atlantic Deep Water (NADW) spreading around 3000 m in the Agulhas-Natal basin. NADW is the oldest water mass found at the Indian-Atlantic Boundary since it was formed in the northern high latitudes before traveling through all the Atlantic basin and finally enter the Indian Ocean south of Africa [*Donohue and Toole*, 2003; *van Aken et al.*, 2004]. This choice is consistent with the profiles of C^{ant} obtained by *Ríos et al.* [2003] and *Lee et al.* [2003] in the eastern South Atlantic where C^{ant} concentrations in NADW are below the detection limit. Note that transient tracers such as CFCs and CCl$_4$ are also below the detection limit in the eastern part of the South Atlantic during the 1990s [*Wallace et al.*, 1994]. The mean ΔC^{0,REF} calculated in the cores of NADW at the Indian-Atlantic boundary is −59 ± 3 μmol/kg [*Lo Monaco et al.*, 2005].

2.3. Comparing Anthropogenic CO$_2$

[21] The three formulations used to estimate C^{ant} can be rearranged as follows so that the three methods become more easily comparable:

$$C^{ant} = DIC - 0.5TA + 0.8O_2 - 0.8TrOCA^0, \qquad (13)$$

$$C^{ant} = DIC - 0.5TA + 0.73O_2 + 0.5TA^0 - 0.73(1 - \alpha k)O_2^{sat} - C^{0,obs} - \Delta C^{0,REF}, \qquad (14)$$

$$C^{ant} = DIC - 0.5TA + 0.73O_2 + 0.5TA^0 - 0.73(1 - \alpha k)O_2^{sat} - C^{eq,280} - \Delta C^{dis}. \qquad (15)$$

The back-calculation methods (equations (14) and (15)) are complex due to the use of predictions to estimate preformed concentrations (O$_2^{sat}$, TA^0 and C^{0,obs}) or DIC in equilibrium with the atmosphere (C^{eq}) and the need of including a correction for oxygen disequilibrium in ice-covered waters (1 − αk). This correction is required in order to avoid a systematic underestimation of C^{ant} (overestimation of C^{bio}) in Antarctic deep and bottom waters formed under the ice from Ice Shelf Water (ISW) and Winter Water (WW). In this study, two potential formation sites must be considered: the Weddell Sea, west of the CIVA-2 transect, and Prydz Bay, east of the transect [e.g., *Schodlok et al.*, 2001]. *Middleton and Humphries*

[1989] showed that similar mixing and thermohaline circulation mechanisms are operating in the Weddell Sea and in Prydz Bay. It is therefore reasonable to consider a mean oxygen disequilibrium (α) as representative of these two formation sites. In the TrOCA method, no assumption is done about oxygen saturation. This means that the oxygen disequilibrium observed in ice-covered surface waters must be implicitly parameterized in equation (13).

[22] When comparing different methods it is important to use the same parameterizations so that differences are only attributed to methodology. However this was not possible here for the Redfield ratios because they are part of the computation of TrOCA^0, ΔC^{0,REF} and ΔC^{dis}. Since we use the TrOCA^0 parameterization estimated by *Touratier and Goyet* [2004b] and ΔC^{dis} values published by *Sabine et al.* [1999], we must keep the same ratios as those used in these studies. *Touratier and Goyet* [2004a, 2004b] choose the C/O$_2$ and N/O$_2$ ratios estimated by *Körtzinger* [2001], giving a coefficient of 0.8 associated with oxygen. *Sabine et al.* [1999] used a coefficient of 0.73 obtained from the ratios estimated by *Anderson and Sarmiento* [1994]. In order to test the sensibility of C^{ant} estimates to different Redfield ratios we performed the C^0 method using either 0.73 or 0.8. We obtained small differences in C^{ant} (<5 μmol/kg) because the impact of changing the Redfield ratios partially cancels out when subtracting the reference term ΔC^{0,REF}. We expect this is also true for the TrOCA method and the ΔC* method.

2.4. Uncertainties and Error Assessment

[23] All three methods are based on the assumption that ocean dynamics and biology as well as air-sea interactions remained unchanged on decadal to centennial timescale. This is also the case when employing ocean models forced with climatologies (e.g., OCMIP1 [*Orr et al.*, 2001]). Regional observations on multidecadal timescale have given evidence that the ocean did not operate at a steady state [e.g., *Wong et al.*, 1999; *Matear et al.*, 2000; *Andreev and Watanabe*, 2002; *Gille*, 2002]. However, large uncertainties are still associated with the long-term variability of ocean processes and the error of C^{ant} estimates when assuming steady state may not be significant if only small changes have occurred in the last centuries. In all three methods it is also assumed that oxygen and alkalinity are not affected by anthropogenic forcing and climate change.

[24] Each method is subjected to random errors from measurements (O$_2$, TA, and DIC) and from predictions (O$_2^{sat}$, TA^0, C^{0,obs}, ΔC^{0,REF}, ΔC^{dis} and TrOCA^0). Table 1 recapitulates the random errors estimated for CIVA-2 data and predictions listed above. A detailed error analysis can be found in *Sabine et al.* [1999], *Lo Monaco et al.* [2005], and *Touratier and Goyet* [2004b]. These analyses show that the random error associated with each parameter listed in Table 1 translates into a relatively small error on C^{ant} estimates: the maximum errors obtained in these studies
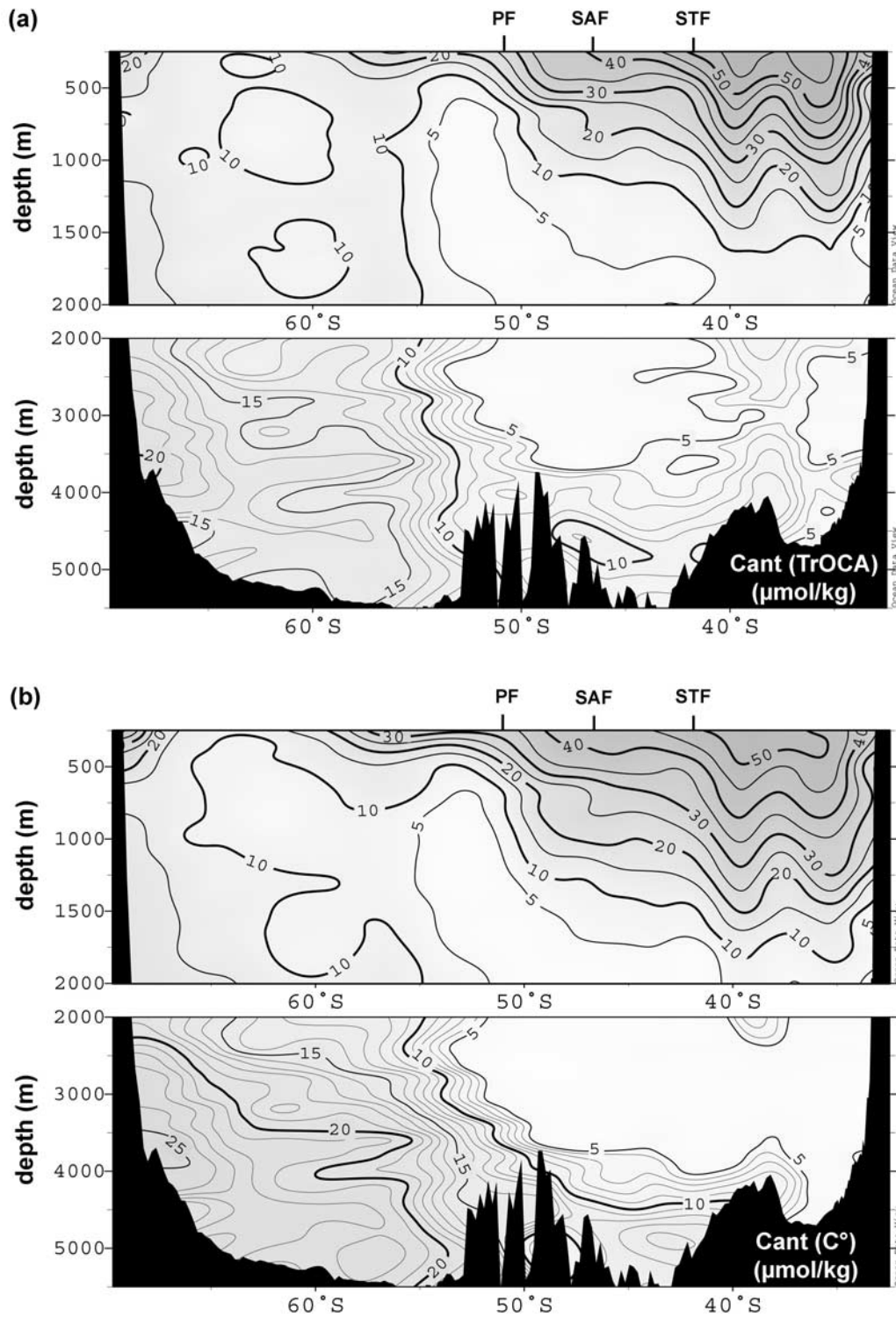
Figure 4. Distribution of anthropogenic CO$_2$ (C^{ant} in μmol/kg) estimated in the Southern Ocean along 30°E (WOCE line I6) using three different methods: (a) the TrOCA method, (b) the preformed DIC (C^0) method, and (c) the ΔC* method.

are 6.1 μmol/kg for the ΔC* method, 6.0 μmol/kg for the C^0 method and 5.9 μmol/kg for the TrOCA method. If the first two estimates could apply in our study, the error given for the original TrOCA method needs to be reevaluated because we use a different parameterization for TrOCA^0.

On the basis of *Touratier and Goyet* [2004b, equation [7]] and random errors estimated in our study (Table 1), we calculated a maximum error of 2.5 μmol/kg for C^{ant} derived from TrOCA. These error analysis do not include systematic errors associated with the choice of the refer-
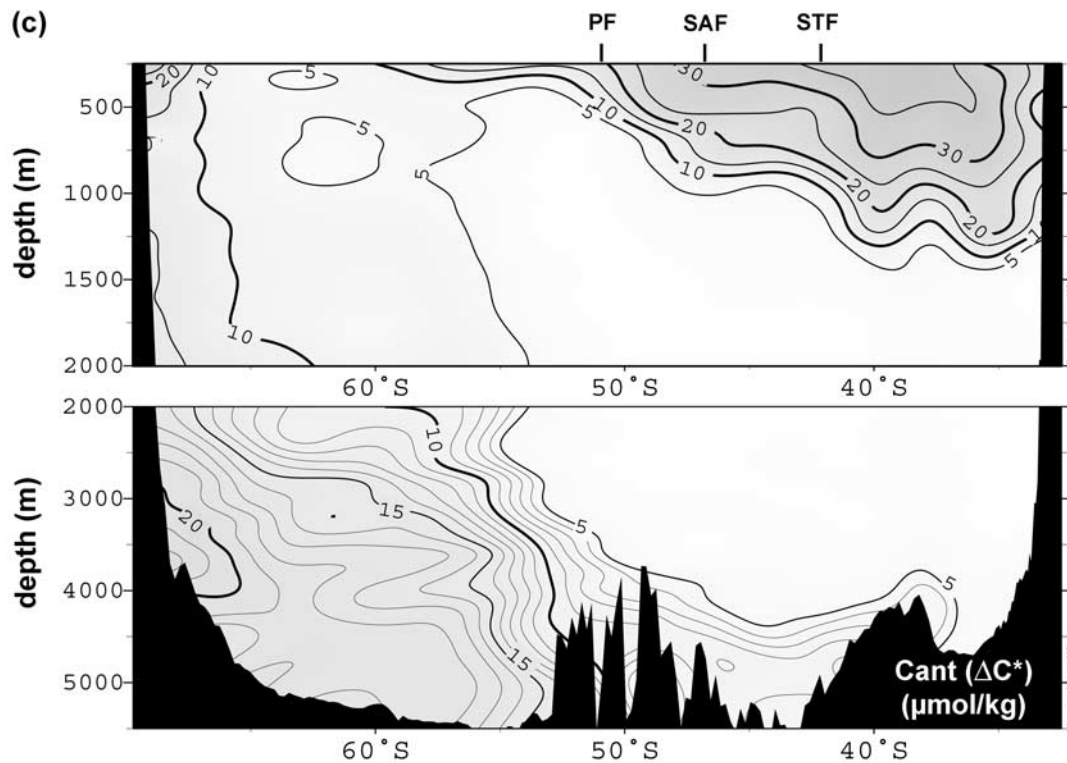
Figure 4. (continued)

ence and C/O$_2$ and N/O$_2$ ratios. As discussed before, the use of different ratios results in small differences in C^{ant} estimates (<5 μmol/kg when using the C^0 method). Concerning the choice of the reference water, the potential systematic error is difficult to asses but clues can be obtained when comparing the distribution of C^{ant} estimated with all three methods since three different reference were used.

3. Results and Discussion

3.1. Distribution of Anthropogenic CO$_2$

[25] Anthropogenic CO$_2$ (C^{ant}) is estimated along 30°E in the Southern Ocean (WOCE line I6, 1996) using the three methods described above: the recently developed TrOCA method and the "historical" C^0 and ΔC* methods corrected for oxygen disequilibrium [Lo Monaco et al., 2005]. The distributions of C^{ant} obtained with these three methods are very similar (Figure 4). In the North, the meandering structure of C^{ant} isolines observed down to 2000 m is generated by the return branch of the Agulhas Current flowing back to the Indian Ocean near 40°S [Gordon, 2003]. A deep penetration of C^{ant} occurs north of the polar front (51°S) down to about 1500 m, associated with the subduction of mode and intermediate waters. The deepest penetration of C^{ant} is found between 35°S and 40°S where mode and intermediate waters converge. Significant concentrations of C^{ant} are also detected in bottom waters flowing north of the Indian-Atlantic ridge (>5 μmol/kg) below the uncontaminated North Atlantic Deep Water (NADW) in the Agulhas-Natal basin. South of 50°S, C^{ant}

concentrations in subsurface waters are lower than in the north due to both the strong stratification of the water column attributed to the presence of Winter Water near 200 m and the upwelling of deep waters with low C^{ant} concentrations. Minimum concentrations are found in the upper Circumpolar Deep Water (upper CDW) lying between 500 and 1000 m. In AABW, C^{ant} concentrations are high both along the Antarctic slope (20–25 μmol/kg) and in the Weddell-Enderby basin (>15 μmol/kg).

[26] The comparison of C^{ant} distributions obtained north of the polar front provides a way to discuss differences among the methods without concern about oxygen disequilibrium. In the northern part of the section, the TrOCA and C^0 methods give very similar response both in term of the magnitude and gradients. The deepening of the 10 μmol/kg C^{ant} isoline toward the north, for example, is in line with the deepening of the 27.5 isopycnal (σ$_\theta$) for both the TrOCA method (down to 1600 m (Figure 4a)) and the C^0 method (down to 1700 m (Figure 4b)). Small differences are observed in the core of AAIW (σ$_\theta$ = 27.1–27.5) where C^{ant} estimates are about 5–7 μmol/kg higher with the C^0 method. Larger differences are found with the ΔC* method whose C^{ant} estimates are always lower than those obtained from the two other methods. In Figure 4c the 10 μmol/kg isoline only reaches 1400 m due to both lower C^{ant} estimates and the sharp gradient observed between isopycnal 27.25 and 27.5. The highest disagreement is found in the lower part of AAIW where C^{ant} estimates are 10 to 20 μmol/kg lower with the ΔC* method. Note however that differences between the ΔC* method and the two other methods are smaller in the upper part of AAIW
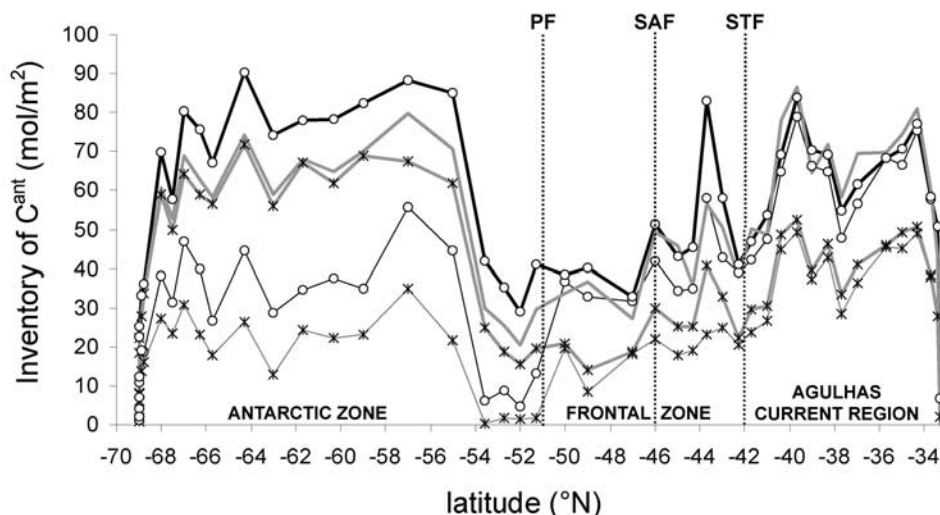
Figure 5. Inventories of anthropogenic CO$_2$ (C^{ant}) estimated in the Southern Ocean along 30°E (WOCE line I6). The inventory obtained with the TrOCA method (shaded bold line) is compared to inventories estimated using the back-calculation methods: C^0 method (black lines and circles) and ΔC* method (shaded lines and star symbols). The back-calculation technique was performed assuming either oxygen equilibrium in all surface waters (thin lines) or 12% undersaturation in ice-covered surface waters (bold lines and symbols).

(between 5 and 10 μmol/kg). It then appears that the ΔC* method gives systematically lower C^{ant} concentrations along shallow isopycnal surfaces, i.e., where the air-sea disequilibrium of CO$_2$ is deduced from CFC-12 data (ΔC*$^{(t)}$ in equation (12)). The limitation of using CFCs as an analog for C^{ant} has been discussed by numerous authors [e.g., *Wallace et al.*, 1994; *Thomas and England*, 2002; *Matear et al.*, 2003]. Here, the main difficulty is that the CFC age method is not straightforward for water masses older than 40 years as found below the 27.25 isopycnal. This is the reason why *Sabine et al.* [1999] used a combination of the mean ΔC*$^{(t)}$ and ΔC*^{,REF} to estimate the CO$_2$ disequilibrium at intermediate density levels. This artifact creates a sharp gradient of C^{ant} near the 27.25 isopycnal where the largest disagreement with the other methods is detected.

[27] In NADW a different pattern is found: the TrOCA method gives slightly higher C^{ant} estimates than the back-calculation methods (about 5 μmol/kg higher). This small offset must be due to the choice of the reference water. We believe that since the two back-calculation methods reach a close agreement in NADW, there might be a systematic error in the computation of TrOCA^0 which would have led to overestimate C^{ant} concentrations in deep waters by about 5 μmol/kg. In the old Circumpolar Deep Water (upper CDW) the TrOCA method also leads to relatively higher C^{ant} when the two back-calculation methods reach a closer agreement.

[28] The comparison of C^{ant} estimates in Antarctic deep and bottom waters shows similar offsets than at midlatitudes: C^{ant} estimates obtained with the TrOCA method stand between those obtained with the C^0 method (the highest) and the ΔC* method (the lowest). These results show that differences exist between C^{ant} estimated from the three different methods, highlighting the methodological uncertainty. An important result is that relatively high

concentrations of C^{ant} are detected with all three methods in AABW flowing along the Antarctic slope, in the Weddell-Enderby basin and below the cores of uncontaminated NADW in the Agulhas-Natal basin. This appears to be coherent with the distribution of CFCs observed along the same line [*Lo Monaco et al.*, 2005]. We believe that since the distributions of C^{ant} present a general agreement, results obtained in this study give the broad picture of what is the real distribution of C^{ant} in the Southern Ocean. The differences observed among the three methods give a taste of the uncertainties attached to C^{ant} inventories.

3.2. Inventories of Anthropogenic CO$_2$

[29] Inventories of C^{ant} are calculated at each station by integrating C^{ant} concentrations from the surface down to the bottom (column inventories). Note that none of the three methods is reliable at the surface and within the mixed layer. However, it is expected that C^{ant} concentrations are rather homogeneous in the mixed layer at least during winter. We therefore assume constant C^{ant} concentrations in the mixed layer and the values calculated at 500 m north of 47°S or 200 m in the south were extended up to the surface. This introduces a potential bias in surface estimates of C^{ant} that should not exceed 10 μmol/kg. Integrating this error over 200 m or 500 m results in a relatively small uncertainty on C^{ant} inventories: about 2 molC/m^2 south of 47°S and 5 molC/m^2 in the north. This systematic error has to be added to the random error associated with C^{ant} estimates: considering a mean signal-to-noise ratio of 30% on C^{ant} concentrations, the random error on C^{ant} inventories ranges between ±18 and ±27 molC/m^2 south of the polar front and between ±6 and ±21 molC/m^2 in the north.

[30] Figure 5 compares the inventories of C^{ant} obtained using all three methods. North of the polar front, inventories of C^{ant} obtained using the ΔC* method are about 20 molC/m^2

lower than those obtained using the TrOCA and C^0 methods. The good agreement obtained between the TrOCA and C^0 methods is the result of a combination of slightly different concentrations in AAIW, NADW and AABW that cancel out each other. In the back-calculation methods, the formulation of the preformed oxygen is corrected in order to take into consideration a mean oxygen undersaturation $\alpha = 12\%$ in ice-covered surface waters. To evaluate the impact of the oxygen saturation correction, we have also performed a standard back-calculation by assuming full equilibrium in surface oxygen ($\alpha = 0$, thin lines in Figure 5). Note that the preformed oxygen correction only has an impact south of the polar front. If the oxygen disequilibrium issue is neglected, inventories of C^{ant} calculated south of the polar front with the back-calculation methods (thin lines) are much lower than inventories estimated using the TrOCA method. In the TrOCA method, no assumption is done about oxygen saturation, thus providing a basis to which back-calculation methods can be compared. When preformed oxygen is corrected for air-sea disequilibrium in ice-covered waters, inventories of C^{ant} increase up to between 60 and 90 molC/m^2, in good agreement with the TrOCA method (shaded bold line).

[31] *Orr et al.* [2001] compared simulations of C^{ant} in four different ocean models. Simulations were performed during the first phase of the Ocean Carbon cycle Model Intercomparison Project (OCMIP1). Inventories of C^{ant} predicted by these models in the Atlantic Ocean show the highest disagreement around 50°N and south of 30°S, in regions where water mass formation occurs (mode, intermediate, deep and bottom waters). Model estimates range between 20 and 40 molC/m^2 in the subtropical/subantarctic band and between 10 and 45 molC/m^2 south of 50°S. In the framework of OCMIP1, ocean model results are compared with inventories of C^{ant} estimated by *Gruber* [1998] using the ΔC* method, which are similar to inventories obtained from the standard ΔC* method use in our study (thin shaded line with star symbols in Figure 5). *Orr et al.* [2001] concluded that all four ocean models overestimate the penetration of C^{ant} in the Southern Ocean. However, when we corrected the preformed oxygen for disequilibrium in ice-covered surface waters, C^{ant} inventories triple south of 50°S up to about 60 molC/m^2 (bold lines), suggesting that all four models might actually underestimate the penetration of C^{ant} in the Southern Ocean.

4. Conclusion

[32] The storage of anthropogenic CO$_2$ into the Southern Ocean was evaluated using three data-based methods: the recently developed TrOCA approach and the "historical" back-calculation methods. A correction is proposed for the back-calculation technique in order to take into account the oxygen disequilibrium observed in surface waters covered with ice. Despite different methodologies, similar results are obtained for both the distribution and the inventory of anthropogenic CO$_2$ at the Indian-Atlantic boundary. The most important result is that larger inventories of anthropogenic CO$_2$ are found in the Antarctic zone (south of 51°S) as compared to the mid latitude region with all three methods. This result is opposed to what was obtained in most previous data-based and model studies. However, it is

coherent with recent results obtained at the Indian-Pacific boundary (WOCE line SR3) showing relatively high anthropogenic CO$_2$ concentrations in bottom waters along the Antarctic slope [*Sabine et al.*, 2002] and a significant increase of excess CO$_2$ on a 28 years period [*McNeil et al.*, 2001]. All these results suggest that the storage of anthropogenic CO$_2$ in the southern high latitudes could be much larger than what is currently believed [e.g., *Sabine et al.*, 2004]. Comparing the data-based distribution and inventories of anthropogenic CO$_2$ with current global model estimates is a next step that will help validate ocean general circulation models used to predict future changes in the ocean carbon sink and how the ocean might impact in a high-CO$_2$ world.

References

Anderson, L. A., and J. L. Sarmiento (1994), Redfield ratios of remineralization determined by nutrient data analysis, *Global Biogeochem. Cycles*, 8, 65–80.

Anderson, L. G., O. Holby, R. Lindegren, and M. Ohlson (1991), The transport of anthropogenic carbon dioxide into the Weddell Sea, *J. Geophys. Res.*, 96, 16,679–16,687.

Andreev, A., and S. Watanabe (2002), Temporal changes in dissolved oxygen of the intermediate water in the subarctic North Pacific, *Geophys. Res. Lett.*, 29(14), 1680, doi:10.1029/2002GL015021.

Benson, B. B., and D. Krause Jr. (1980), The concentration and isotopic frationation of gases dissolved in fresh water in equilibrium with the atmosphere, *Limnol. Oceanogr.*, 25, 662–671.

Bopp, L., P. Monfray, O. Aumont, J.-L. Dufresne, H. Le Treut, G. Madec, L. Terray, and J. C. Orr (2001), Potential impact of climate change on marine export production, *Global Biogeochem. Cycles*, 15, 81–99.

Brewer, P. G. (1978), Direct observation of the oceanic CO$_2$ increase, *Geophys. Res. Lett.*, 5, 997–1000.

Broecker, W. S. (1974), "NO" a conservative water-mass tracer, *Earth Planet. Sci. Lett.*, 23, 100–107.

Chen, C. T. A. (1982), On the distribution of anthropogenic CO$_2$ in the Atlantic and Southern Oceans, *Deep Sea Res.*, 29, 563–580.

Chen, C. T. A. (1993), The oceanic anthropogenic CO$_2$ sink, *Chemisphere*, 27, 1041–1064.

Chen, C. T. A., and F. J. Millero (1979), Gradual increase of oceanic CO$_2$, *Nature*, 277, 205–206.

Coatanoan, C., N. Metzl, M. Fieux, and B. Coste (1999), Seasonal water mass distribution in the Indonesian throughflow entering the Indian Ocean, *J. Geophys. Res.*, 104, 20,801–20,826.

Donohue, K. A., and J. M. Toole (2003), A near-synoptic survey of the southwest Indian Ocean, *Deep Sea Res.*, 50, 1893–1931.

Friedlingstein, P., J.-L. Dufresne, P. M. Cox, and P. Rayner (2003), How positive is the feedback between climate change and the carbon cycle?, *Tellus, Ser. B*, 55, 692–700.

Gibson, J. A. E., and T. W. Trull (1999), Annual cycle of fCO$_2$ under sea-ice and in open water in Prydz Bay, east Antarctica, *Mar. Chem.*, 66, 187–200.

Gille, S. (2002), Warming of the Southern Ocean since the 1950s, *Science*, 295, 1275–1277.

Gordon, A. L. (2003), Oceanography: The brawniest retroflection, *Nature*, 421, 904–905.

Goyet, C., R. Adams, and G. Eischeid (1998), Observed increase of anthropogenic CO$_2$ in the tropical Atlantic Ocean, *Mar. Chem.*, 60, 49–61.

Goyet, C., C. Coatanoan, G. Eischeid, T. Amaoka, K. Okuda, R. Healy, and S. Tsunogai (1999), Spatial variation of total CO$_2$ and total alkalinity in the northern Indian Ocean: A novel approach for the quantification of anthropogenic CO$_2$ in seawater, *J. Mar. Res.*, 57, 135–163.

Gruber, N. (1998), Anthropogenic CO$_2$ in the Atlantic Ocean, *Global Biogeochem. Cycles*, 12, 165–191.

Gruber, N., J. L. Sarmiento, and T. F. Stocker (1996), An improved method for detecting anthropogenic CO$_2$ in the oceans, *Global Biogeochem. Cycles*, *10*, 809–837.

Hall, T. M., D. W. Waugh, T. W. N. Haine, P. E. Robbins, and S. Khatiwala (2004), Estimates of anthropogenic carbon in the Indian Ocean with allowance for mixing and time-varying air-sea CO$_2$ disequilibrium, *Global Biogeochem. Cycles*, *18*, GB1031, doi:10.1029/2003GB002120.

Holfort, J., K. M. Johnson, B. Schneider, G. Siedler, and D. W. R. Wallace (1998), Meridional transport of dissolved inorganic carbon in the South Atlantic Ocean, *Global Biogeochem. Cycles*, *12*, 479–499.

Ito, T., M. J. Follows, and E. A. Boyle (2004), Is AOU a good measure of respiration in the oceans?, *Geophys. Res. Lett.*, *31*, L17305, doi:10.1029/2004GL020900.

Körtzinger, A. (2001), Redfield ratios revisited: Removing the biasing effect of anthropogenic CO$_2$, *Limnol. Oceanogr.*, *46*, 964–970.

Körtzinger, A., L. Mintrop, and J. C. Duinker (1998), On the penetration of anthropogenic CO$_2$ into the North Atlantic Ocean, *J. Geophys. Res.*, *103*, 18,681–18,689.

Körtzinger, A., M. Rhein, and L. Mintrop (1999), Anthropogenic CO$_2$ and CFCs in the North Atlantic Ocean: A comparison of man-made tracers, *Geophys. Res. Lett.*, *26*, 2065–2068.

Lee, K., et al. (2003), An updated anthropogenic CO$_2$ inventory in the Atlantic Ocean, *Global Biogeochem. Cycles*, *17*(4), 1116, doi:10.1029/2003GB002067.

Lo Monaco, C., N. Metzl, A. Poisson, C. Brunet, and B. Schauer (2005), Anthropogenic CO$_2$ in the Southern Ocean: Distribution and inventory at the Indian-Atlantic boundary (World Ocean Circulation Experiment line I6), *J. Geophys. Res.*, *110*, C06010, doi:10.1029/2004JC002643.

Mantisi, F., C. Beauverger, A. Poisson, and N. Metzl (1991), Chlorofluoromethanes in the western Indian sector of the Southern Ocean and their relations with geochemical tracers, *Mar. Chem.*, *35*, 151–167.

Matear, R. J., A. C. Hirst, and B. I. McNeil (2000), Changes in dissolved oxygen in the Southern Ocean with climate change, *Geochem. Geophys. Geosyst.*, *1*, doi:10.1029/2000GC000086.

Matear, R. J., C. S. Wong, and L. Xie (2003), Can CFCs be used to determine anthropogenic CO$_2$?, *Global Biogeochem. Cycles*, *17*(1), 1013, doi:10.1029/2001GB001415.

McNeil, B. I., B. Tilbrook, and R. J. Matear (2001), Accumulation and uptake of anthropogenic CO$_2$ in the Southern Ocean, south of Australia between 1968 and 1996, *J. Geophys. Res.*, *106*, 31,431–31,445.

Middleton, J. H., and S. E. Humphries (1989), Thermohaline structure and mixing in the region of Prydz Bay, Antarctica, *Deep Sea Res., Part A*, *36*, 1255–1266.

Orr, J. C., et al. (2001), Estimates of anthropogenic carbon uptake from four three-dimensional global ocean models, *Global Biogeochem. Cycles*, *15*, 43–60.

Orsi, A. H., W. M. Smethie Jr., and J. L. Bullister (2002), On the total input of Antarctic waters to the deep ocean: A preliminary estimate from chlorofluorocarbon measurements, *J. Geophys. Res.*, *107*(C8), 3122, doi:10.1029/2001JC000976.

Pérez, F. F., M. Álvarez, and A. F. Ríos (2002), Improvements on the back-calculation technique for estimating anthropogenic CO$_2$, *Deep Sea Res., Part I*, *49*, 859–875.

Poisson, A., and C. T. A. Chen (1987), Why is there little anthropogenic CO$_2$ in Antarctic Bottom Water?, *Deep Sea Res.*, *34*, 1255–1275.

Rintoul, S. R., C. W. Hughes, and D. Olbers (2001), The Antarctic Circumpolar Current system, in *Ocean Circulation and Climate*, edited by G. Siedler, J. Church, and J. Gould, pp. 489–520, Elsevier, New York.

Ríos, A. F., X. A. Álvarez-Salgado, F. F. Pérez, L. S. Bingler, J. Arístegui, and L. Mémery (2003), Carbon dioxide along WOCE line A14: Water masses characterization and anthropogenic entry, *J. Geophys. Res.*, *108*(C4), 3123, doi:10.1029/2000JC000366.

Sabine, C. L., and R. A. Feely (2001), Comparison of recent Indian Ocean anthropogenic CO$_2$ estimates with a historical approach, *Global Biogeochem. Cycles*, *15*, 31–42.

Sabine, C. L., R. M. Key, K. M. Johnson, F. J. Millero, A. Poisson, J. L. Sarmiento, D. W. R. Wallace, and C. D. Winn (1999), Anthropogenic CO$_2$ inventory of the Indian Ocean, *Global Biogeochem. Cycles*, *13*, 179–198.

Sabine, C. L., R. A. Feely, R. M. Key, J. L. Bullister, F. J. Millero, K. Lee, T.-H. Peng, B. Tilbrook, T. Ono, and C. S. Wong (2002), Distribution of anthropogenic CO$_2$ in the Pacific Ocean, *Global Biogeochem. Cycles*, *16*(4), 1083, doi:10.1029/2001GB001639.

Sabine, C. L., et al. (2004), The oceanic sink for anthropogenic CO$_2$, *Science*, *305*, 367–371.

Schodlok, M. P., C. B. Rodehacke, H. H. Hellmer, and A. Beckmann (2001), On the origin of the deep CFC maximum in the eastern Weddell Sea: Numerical model results, *Geophys. Res. Lett.*, *28*, 2859–2862.

Shiller, A. M. (1981), Calculating the oceanic CO$_2$ increase: A need for caution, *J. Geophys. Res.*, *86*, 11,083–11,088.

Shiller, A. M. (1982), Reply, *J. Geophys. Res.*, *87*, 2086.

Thomas, H., and M. H. England (2002), Different oceanic features of anthropogenic CO$_2$ and CFCs, *Naturwissenschaften*, *89*, 399–403.

Tomczak, M. (1981), A multi-parameter extension of temperature/salinity diagram techniques for the analysis of non-isopycnal mixing, *Prog. Oceanogr.*, *10*, 147–171.

Touratier, F., and C. Goyet (2004a), Definition, properties, and Atlantic Ocean distribution of the new tracer TrOCA, *J. Mar. Syst.*, *46*, 169–179.

Touratier, F., and C. Goyet (2004b), Applying the new TrOCA approach to estimate the distribution of anthropogenic CO$_2$ in the Atlantic Ocean, *J. Mar. Syst.*, *46*, 181–197.

van Aken, H. M., H. Ridderinkhof, and W. P. M. de Ruijter (2004), North Atlantic deep water in the south-western Indian Ocean, *Deep Sea Res., Part I*, *51*, 755–776.

Wallace, D. W. R. (2001a), Introduction to special section: Ocean measurements and models of carbon sources and sinks, *Global Biogeochem. Cycles*, *15*, 3–10.

Wallace, D. W. R. (2001b), Storage and transport of excess CO$_2$ in the oceans: The JGOFS/WOCE global CO$_2$ survey, in *Ocean Circulation and Climate*, edited by G. Siedler, J. Church, and J. Gould, pp. 489–520, Elsevier, New York.

Wallace, D. W. R., P. Beining, and A. Putzka (1994), Carbon tetrachloride and chlorocarbons in the South Atlantic Ocean, 19°S, *J. Geophys. Res.*, *99*, 7803–7819.

Wanninkhof, R., S. C. Doney, T.-H. Peng, J. L. Bullister, K. Lee, and R. A. Feely (1999), Comparison of methods to determine the anthropogenic CO$_2$ invasion into the Atlantic Ocean, *Tellus, Ser. B*, *51*, 511–530.

Watson, A. J., D. C. E. Bakker, A. J. Ridgwell, P. W. Boyd, and C. S. Law (2000), Effect of iron supply on Southern Ocean CO$_2$ uptake and implications for glacial atmospheric CO$_2$, *Nature*, *407*, 730–734.

Weiss, R. F., H. G. Östlund, and H. Craig (1979), Geochemical studies of the Weddell Sea, *Deep Sea Res., Part A*, *26*, 1093–1120.

Wong, A. P. S., N. L. Bindoff, and A. Forbes (1998), Ocean-ice shelf interaction and possible bottom water formation in Prydz Bay, Antarctica, *Antarct. Res. Ser.*, *75*, 173–187.

Wong, A. P. S., N. L. Bindoff, and J. A. Church (1999), Large-scale freshening of intermediate waters in the Pacific and Indian Oceans, *Nature*, *400*, 440–443.

————————————

C. Goyet and F. Touratier, Laboratoire de Biophysique et Dynamique des Systèmes Intégrés, Université de Perpignan, F-66860 Perpignan, France. (cgoyet@univ-perp.fr; touratie@univ-perp.fr)

C. Lo Monaco, N. Metzl, and A. Poisson, Laboratoire d'Océanographie et du Climat: Expérimentations et Approches Numériques, Université Pierre et Marie Curie, case 134, 4 place Jussieu, F-75252 Paris Cedex 5, France. (lomonaco@ccr.jussieu.fr; metzl@ccr.jussieu.fr; apoisson@ccr.jussieu.fr)